Polymer Chemistry

PAPER

View Article Online
View Journal | View Issue

Check for updates

Cite this: *Polym. Chem.*, 2017, **8**, 2997

A pH, glucose, and dopamine triple-responsive, self-healable adhesive hydrogel formed by phenylborate–catechol complexation†

Meng Shan,‡ Chu Gong,‡ Bingqiang Li and Guolin Wu *

Received 28th March 2017,
Accepted 12th April 2017

DOI: 10.1039/c7py00519a

rsc.li/polymers

An injectable polyethylene glycol (PEG) hydrogel was successfully prepared *via* borate–catechol complexation using dopamine functionalized 4-armed PEG (4-arm-PEG-DA) and phenylboronic acid modified 4-armed PEG (4-arm-PEG-PBA). The hydrogel was formed within 10 s by mixing 15 wt% 4-arm-PEG-DA with 15 wt% 4-arm-PEG-PBA buffer solutions at pH 9.0. The hydrogel was characterized by Fourier transform infrared (FT-IR) spectroscopy, rheological measurements, scanning electron microscopy (SEM) and lap shear strength tests. Furthermore, pH, glucose and dopamine responsiveness of the hydrogel based on phenylborate–catechol complexation was demonstrated by degradation experiments and drug release tests. The lap shear strength tests indicated that the hydrogel possessed the ability of self-healing which was bestowed by the phenylborate–catechol dynamic covalent bond. Moreover, the hydrogel could serve as a decent bio-adhesive due to its adhesion properties on different substrates especially the porcine skin. *In vitro* cytotoxicity tests demonstrated the excellent cytocompatibility of the hydrogel. The results of all the experiments indicate that our newly developed multi-functionalized hydrogel can have potential applications in biomedical fields such as drug delivery, tissue engineering, and bio-adhesives.

Published on 13 April 2017. Downloaded on 10/1/2025 12:23:07 AM.

1. Introduction

Hydrogels are three-dimensional polymeric networks with high water content similar to tissues. Their applications in many areas of medicine, particularly, tissue engineering, surgery, and drug release have attracted significant attention.[1–3] In recent years, stimuli-responsive hydrogels have been in great demand in medical fields due to their unique properties.[4] Some hydrogels showing response to pH,[5] temperature,[6] and light[7] have been reported.

Phenylborate ester is formed by phenylboric acid and vicinal diol in alkaline environment, which is not stable under acidic conditions. Therefore, phenylborate ester bonds can bestow pH-responsiveness on materials. A phenylborate–catechol crosslinked hydrogel formed by branched catechol derivatized poly(ethyleneglycol) (cPEG) with 1,3-benzenediboronic acid has been reported[1] to exhibit pH-responsiveness. However, the disadvantages of these materials such as a long gelation time and difficulty in adjusting the proportion of precursor solutions need to be addressed. The most commonly used vicinal diols to construct hydrogels based on phenylborate ester bonds are saccharide derivatives.[8–10]

pH-Sensitive hydrogels have potential applications in drug delivery. The low pH of some tissues can trigger the release of the loaded drug in hydrogels to achieve the goal of the treatment.[11–13] Glucose-responsive hydrogels can improve the traditional insulin therapy for diabetes, which is not able to regulate the blood glucose level precisely.[14,15] Some mental diseases such as Parkinson's and Alzheimer disease have a close relationship with an abnormal dopamine level. Dopamine-responsive hydrogels that have not been reported are believed to have a promising prospect in treating mental diseases.

Hydrogels with self-healing ability are highly desirable in extending their life span under some conditions. Natural hydrogels such as bio-tissues (*e.g.* heart valves) belong to the category of excellent self-healable materials to some extent.[16,17] The self-healable hydrogels are commonly designed using physical interactions, coordination,[5] or dynamic covalent bonds. Polyrotaxane hydrogel is one of the examples of self-healing hydrogels based on physical interactions.[18–20] The research has shown that the reversible slide-ring structure is crucial to achieve their self-healing abilities. The nonco-

Key Laboratory of Functional Polymer Materials, Institute of Polymer Chemistry, Nankai University, Tianjin 300071, P. R. China. E-mail: guolinwu@nankai.edu.cn; Fax: +86 22 23502749; Tel: + 86 22 23507746

†Electronic supplementary information (ESI) available. See DOI: 10.1039/c7py00519a

‡These authors contributed equally to this paper.

Published on 13 April 2017. Downloaded on 10/1/2025 12:23:07 AM.

valent interactions such as metal–catechol coordination inspired from mussel adhesive proteins can spontaneously reform after breaking, also providing the self-healing ability to materials. The catechol groups are capable of forming strong complexes with metal ions such as Fe^{3+}, whose coordination modes (mono-, bis-, and tris-complexes) strongly depend on the pH value and the ion valence. Fe^{3+} complexes possess the highest stability constants among some known metal–ligand chelates and additionally, a hydrogel based on catechol–Fe^{3+} interactions has also exhibited an excellent self-healing ability.[5,21,22] The hydrogels constructed *via* dynamic covalent chemistry are extremely promising and also ahead of noncovalent hydrogels in the aspect of mechanical strength and stability.[1,16] Different types of dynamic covalent bonds such as phenylborate ester bonds,[1,23,24] acylhydrazone bonds,[25] disulfide bonds,[26] and Diels–Alder reactions[27] have been utilized to design self-healing hydrogels. In these dynamic covalent bonds, as previously mentioned, the stability of the phenylborate ester bond is significantly dependent on pH. It has been demonstrated that the complexation of phenylboric acid with vicinal diol only occurs at pH values above the diol pK_a values.[1,14]

Phenylboronic acid (PBA) and its derivatives have been widely applied in glucose-responsive materials as insulin delivery systems for the treatment of diabetes. Kataoka *et al.*[23] prepared a hydrogel composed of poly(*N*-isopropylacrylamide) (PNIPAM) with phenylboronic acid moieties undergoing an abrupt change in the degree of swelling at a critical glucose concentration. The on–off regulated release of insulin was achieved in this system. Guan *et al.*[24] summarized the strategies for the design and synthesis of various boronic acid-containing hydrogels as well as their properties and applications in glucose sensing and self-regulated insulin release.

Robust adhesion is one of the most important requirements of biomedical adhesives. However, the applications of current commercial adhesives such as fibrin glue or cyanoacrylates have been restricted due to some aspects such as low bonding strength with tissues and toxic degradation products.[6,28,29] Some improvements of these adhesives are in great demand for extending their applications. Marine mussels are known to adhere onto various substrates like organic/inorganic surfaces under wet conditions because the abundant 3,4-dihydroxy-phenylalanine (DOPA) residues in mussel adhesive proteins can form noncovalent bonds with ions or strong covalent bonds with various groups including thiol and amine *via* Michael-type additions or Schiff base reactions, respectively.[30–36] The development of a new adhesive hydrogel inspired by the mussel adhesion mechanism seems promising in order to overcome the limitations of conventional tissue adhesives.[33–35]

In the current research work, we report a hydrogel formulated *via* reversible covalent phenylborate ester bonds between 4-arm-PEG-DA and 4-arm-PEG-PBA. The self-healable PEG hydrogel has pH, glucose, and dopamine triple responsiveness and its robust adhesive properties also render it with a great potential to be used as an excellent bio-adhesive.

2. Experiment

2.1. Materials

4-Arm-poly(ethylene glycol)-succinimide glutaric acid ester (4-arm-PEG-SG) (M_w = 10 000) and 4-arm-poly(ethylene glycol)-amine (4-arm-PEG-NH_2) (M_w = 10 000) were obtained from Changsha PassKey Instrument Co. Ltd. Dopamine hydrochloride (99%), *N*,*N*′-dicyclohexylcarbodiimide (DCC) (98%) and rhodamine B (90%) were purchased from Tianjin HEOWNS Biochemical Technology Co. Ltd. Methylene blue and D-(+)-glucose (≥99.5%) were supplied by Aladdin. 4-Carboxylphenylboronic acid pinacol ester (98%) was purchased from Energy Chemical. Other reagents were obtained from Tianjin Chemical Reagent Company.

2.2. Synthesis of dopamine-functionalized 4-arm-PEG (4-arm-PEG-DA)

4-Arm-PEG-DA was prepared *via* the nucleophilic substitution reaction between 4-arm-PEG-SG and dopamine. Briefly, 4-arm-PEG-SG (1.0 g, 0.1 mmol) and dopamine hydrochloride (0.11 g, 0.6 mmol) were dissolved in 5 mL of dimethyl sulfoxide (DMSO). Thereafter, trimethylamine (83 μL, 0.6 mmol) was added dropwise to the solution to neutralize the hydrochloride. The mixture was stirred at room temperature under a nitrogen atmosphere for three days. The reaction solution was extracted three times with 15 mL (5 mL × 3) of dichloromethane (CH_2Cl_2) and 15 mL of saturated sodium chloride solution (NaCl-saturated). The organic phase was further purified three times with 150 mL (50 mL × 3) of saturated NaCl. Subsequently, the organic phase was concentrated and precipitated into excess diethyl ether. The precipitate was further washed three times with diethyl ether and dried under vacuum at room temperature for 24 h to obtain the final product, dopamine-terminated 4-arm-PEG (4-arm-PEG-DA, yield: 90%).

2.3. Synthesis of phenylboronic acid-functionalized 4-arm-PEG (4-arm-PEG-PBA)

4-Arm-PEG-PBA was synthesized through a condensation reaction between 4-arm-PEG-NH_2 and 4-carboxylphenylboronic acid pinacol ester. In brief, 4-arm-PEG-NH_2 (1.0 g, 0.1 mmol) and 4-carboxylphenylboronic acid pinacol ester (212 mg, 0.8 mmol) were dissolved in 6 mL of CH_2Cl_2. The condensation agent DCC (172 mg, 0.83 mmol) dissolved in 2 mL of CH_2Cl_2 was added dropwise to the mixture and the reaction was conducted for one day at room temperature under constant stirring. After the reaction duration of 10 min, a white precipitate appeared, which was the by-product of DCC, namely, dicyclohexylurea (DCU).[37] The final reaction mixture was firstly filtered to remove DCU and the filtrate was precipitated into excess diethyl ether. The obtained precipitate was dissolved in 10 mL of deionized water and the pH was adjusted to 1 using hydrochloric acid (HCl). The product was dialyzed (MWCO: 3500 Da) against deionized water for two days and additionally lyophilized, yielding the final product, phenylboronic acid-functionalized (4-arm-PEG-PBA, yield: 85%).

 This journal is © The Royal Society of Chemistry 2017

Published on 13 April 2017. Downloaded on 10/1/2025 12:23:07 AM.

2.4. Hydrogel preparation

Hydrogels were prepared by mixing 15 wt% 4-arm-PEG-DA and 15 wt% 4-arm-PEG-PBA boronic acid buffer (pH 9.0, 10 mM) solutions of equal volume proportion at 37 °C. The gelation time was determined when the mixture ceased flowing in an inverted vial.[12,38]

2.5. Polymer and hydrogel characterization

4-Arm-PEG-DA and 4-arm-PEG-PBA were characterized by ^{1}H nuclear magnetic resonance (^{1}H-NMR) (Bruker Avance, 400 MHz) using $CDCl_3$ as the solvent. The chemical shifts were reported in ppm. FT-IR (Bio-Rad FTS6000) spectra were recorded at room temperature. The samples were mixed with KBr powder by grinding followed by compressing the mixture to form a pellet. Since, the freeze-dried hydrogel was difficult to grind, the PEG hydrogel was characterized by attenuated total reflectance-Fourier transform infrared (ATR-FT-IR) spectroscopy.[39–41]

2.6. pH responsive degradation of hydrogels

Initially, hydrogels (0.2 g) were prepared by mixing 100 μL of 4-arm-PEG-DA solutions (15 wt%) and 100 μL of 4-arm-PEG-PBA solutions (15 wt%) at pH 9.0. Then hydrogels were immersed in buffers at different pH, namely, boronic acid buffer (pH 9.0, 10 mM), PBS (pH 7.4, 10 mM), acetate buffer (pH 5.0, 10 mM) and citrate buffer (pH 3.0, 10 mM) at 37 °C and weighed at selected time points. The final data were recorded as mean ± SD (n = 3).

2.7. Glucose responsive degradation of hydrogels

The hydrogels (0.2 g) were prepared as mentioned above. Glucose was dissolved in PBS (pH 7.4, 10 mM) to prepare solutions at concentrations of 0.9 and 9 mg mL^{-1}, respectively. Thereafter, the hydrogels were immersed in PBS solutions of glucose at 37 °C and weighed at certain time points. The final data were recorded as mean ± SD (n = 3).

2.8. Dopamine responsive degradation of hydrogels

The hydrogels (0.2 g) were prepared as mentioned above. Dopamine hydrochloride was dissolved in PBS (pH 7.4, 10 mM) to prepare solutions at concentrations of 0.01, 0.1, 1 and 10 mM. Thereafter, the hydrogels were immersed in PBS solutions of dopamine at different concentrations at 37 °C and weighed at certain time points. The final data were recorded as mean ± SD (n = 3).

2.9. Rheological behavior of hydrogels

The viscoelastic properties of hydrogels were investigated using a rheometer (TA AR2000ex). The elastic modulus (G') and viscous modulus (G'') were measured as a function of angular frequency at 25 °C. In the current research work, the volume of hydrogel precursor solutions was kept at 1 mL in total to ensure that the rheometer plate was paved with a hydrogel with a thickness of 3 mm.

2.10. Cross-sectional morphology of hydrogels

The cross-sectional morphology of the lyophilized hydrogel was observed by SEM (QUANTA 200) with an accelerating voltage of 15 kV, working distance of 9.9 mm and magnification of 600 and 1200. For the preparation of samples, the hydrogels were freeze-dried and then the cross section was gold-coated before observation.

2.11. Self-healing properties of hydrogels

The PEG hydrogel exhibited self-healing properties due to the reversible and dynamic phenylborate ester bonds, which were verified *via* fracture and reformation of hydrogels. In brief, the hydrogel (0.6 g) was cut into two pieces and one piece was dyed with methylene blue for convenient observation.[14] Then the fractured surfaces of the two pieces were brought into contact with each other to observe the self-healing phenomenon.

2.12. *In vitro* release of rhodamine B from the hydrogels

Rhodamine B was dissolved in boronic acid buffer (pH 9.0, 10 mM) to reach a final concentration of 0.3 mg mL^{-1}. In the next step, hydrogels (0.2 g) were prepared using the boronic acid buffer containing rhodamine B as the solvent. Thereafter, the hydrogels were sealed in dialysis bags (MWCO: 3500 Da) and immersed in centrifuge tubes containing 20 mL of different buffers (buffers at different pH values (pH 9.0, 7.4 and 5.0), PBS solutions of glucose at a concentration of 0.9 mg mL^{-1}, and PBS solutions of dopamine at a concentration of 0.01 mM). The centrifuge tubes were placed in a shaking bed at 37 °C. 3 mL of the release media was taken out at specific time intervals and replaced with 3 mL of the corresponding fresh solutions. The rhodamine B concentration was determined by an ultraviolet-visible (UV-vis) spectrophotometer (UV-2450, Shimadzu, Japan). The cumulative release of rhodamine B (%) was calculated according to the following formula:

$$\text{Cumulative release of rhodamine B (\%)} = \frac{V_e \sum_{1}^{n-1} C_i + V_0 C_n}{m_0} \times 100\%$$

where V_e is the amount of release medium removed at a certain time (3 mL), V_0 is the total amount of the original volume (20 mL), C_i is the concentration of rhodamine B released from the hydrogel at a displacement time of i, n is the displacement time and m_0 is the total mass of rhodamine B in the hydrogel. The final data were recorded as mean ± SD (n = 3).

2.13. Lap shear adhesion tests

Porcine skins were purchased from a local slaughterhouse immediately after their death. Dry porcine skin substrates were cut into pieces with an area of 2.5 cm × 3 cm and rehydrated for 1 h in PBS at 37 °C.[12,13,42–44] The tissue substrates were immobilized on clear glass slides (25.4 × 76.2 mm) using a cyanoacrylate glue (gold elephant 508) and allowed to cure for 1 h before adhesive hydrogel deposition. The hydrogel (0.6 g) was

Published on 13 April 2017. Downloaded on 10/1/2025 12:23:07 AM.

applied to one end of a piece of porcine skin and was spread by using the tip of a pipette. Subsequently, the adhesive joint was formed by placing the second piece of porcine skin over the first one, generating a single test sample. The adhesive joint was compressed with a weight of 100 g for 30 min. The area of the substrate overlap was measured using digital calipers immediately before testing.[42,43] The samples were pulled till failure using a universal testing machine (UTM, Shenzhen Suns Technology Stock Co. Ltd) at a rate of 5 mm min^{-1}. The samples were pulled until the tissues separated, and the maximum load and displacement were recorded. The shear strength was determined by dividing the maximum load by the initial area of the adhesive overlap. Thereafter, the hydrogels after self-healing were also tested to differentiate from the original sample. Additionally, glass slides (25.4 × 76.2 mm) as another substrate were tested using the same method as well. At least five parallel samples were tested in each group.

2.14. *In vitro* cytotoxicity tests

The cytotoxicity was evaluated by determining the viability of cells exposed to the hydrogel extracts using a quantitative 3-(4,5-dimethyl-2-thiazolyl)-2,5-diphenyl-2-*H*-tetrazolium bromide (MTT) assay.[43,45,46] The sterile hydrogel (1 g) was immersed in 5 mL of PBS and hydrogel extracts were prepared at 1 h, 4 h, 10 h and 24 h, respectively. L929 mouse fibroblasts were seeded into a 96-well microculture plate at a density of 1×10^4 cells per well and incubated for 24 h at 37 °C in a 5% CO_2 humidified incubator to obtain a confluent monolayer of cells. Thereafter, hydrogel extracts prepared at 1 h, 4 h, 10 h, and 24 h were added into the well. Each dosage was replicated in 6 wells. After further incubation for 48 h, the hydrogel extracts were removed and the cells were incubated with 50 μL of MTT (1 mg mL^{-1}) for 2 h. Finally, the solution was removed and 100 μL of DMSO was added to dissolve formazan. The absorbance of each well was measured at a wavelength of 570 nm using a microplate reader (Lab-system, Multiskan, Ascent, Model 354 Finland). The relative cell viability was calculated according to the ratio of the mean absorbance values of the sample and the mean absorbance value of negative control (PBS). The positive control was 1% triton X-100. The samples with a relative cell viability of less than 70% are deemed to be cytotoxic.[43,47] L929 mouse fibroblasts were provided by the Institute of Radiation Medicine, Chinese Academy of Medical Sciences.

2.15. Cell growth on the surface of hydrogels

In order to further evaluate the biocompatibility of hydrogels, the cell growth on the surface of PEG hydrogels was observed. In brief, hydrogels were prepared in a 24-well plate and then L929 cells were seeded on the surface of hydrogels at a density of 1×10^4 cells per well in DMEM complete medium, followed by incubation at 37 °C in a 5% CO_2 humidified incubator. After incubation for 0, 1 and 2 days, the acridine orange/ethidium bromide (AO/EB) stain was added and then the fluorescence images of the cells were observed using an inverted fluorescence microscope (Nikon INTENSILIGHT, C-HGFI).

3. Results and discussion

3.1. Synthesis and characterization of polymers

Scheme 1 illustrates the synthetic route for the preparation of 4-arm-PEG-DA and 4-arm-PEG-PBA. The backbone was PEG providing both hydrophilicity and biocompatibility. Scheme 2 is the illustration of the formation of PEG hydrogels through phenylborate ester bonds. PEG hydrogels were formed (Fig. 1) within 10 s through the complexation between catechol and phenylboronic acid.

Fig. 2A and B show the ^{1}H-NMR spectra of 4-arm-PEG-DA and 4-arm-PEG-PBA, respectively. The appearance of peaks at 6.5 (a), 6.7 (b) and 6.8 (c) ppm in Fig. 2A indicates the success-

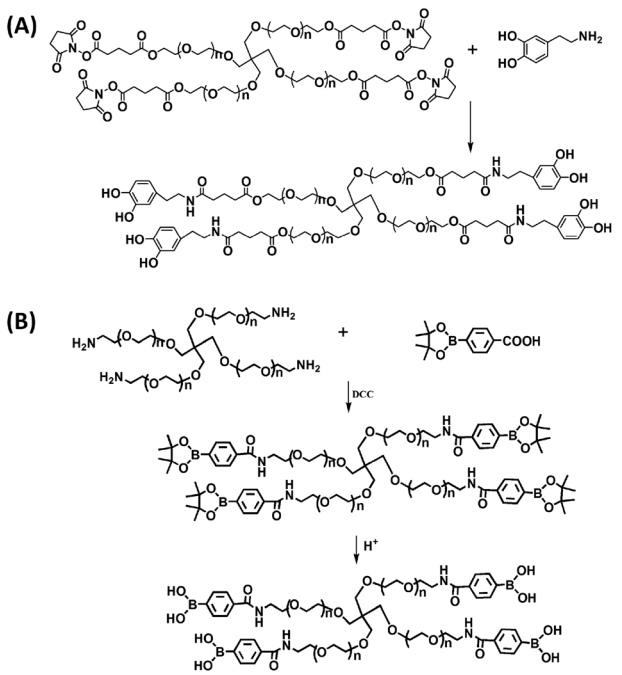

Scheme 1 The synthetic route for 4-arm-PEG-DA (A) and 4-arm-PEG-PBA (B).

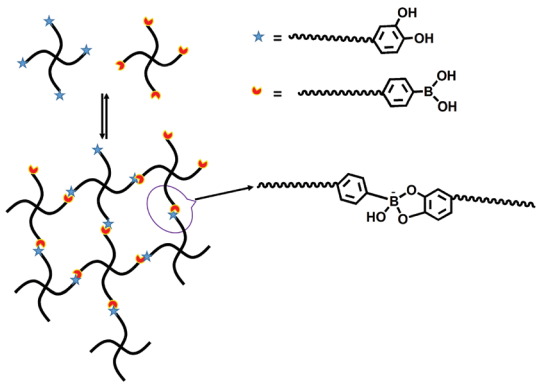

Scheme 2 The schematic illustration of 4-arm-PEG-DA (blue), 4-arm-PEG-PBA (red) and PEG hydrogel.

 This journal is © The Royal Society of Chemistry 2017

Published on 13 April 2017. Downloaded on 10/1/2025 12:23:07 AM.

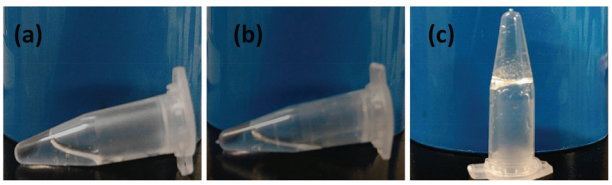

Fig. 1 Photograph of the final transparent hydrogel (c), which was formed within 10 s by mixing 15 wt% 4-arm-PEG-DA (a) and 15 wt% 4-arm-PEG-DA (b) solutions at pH 9.0.

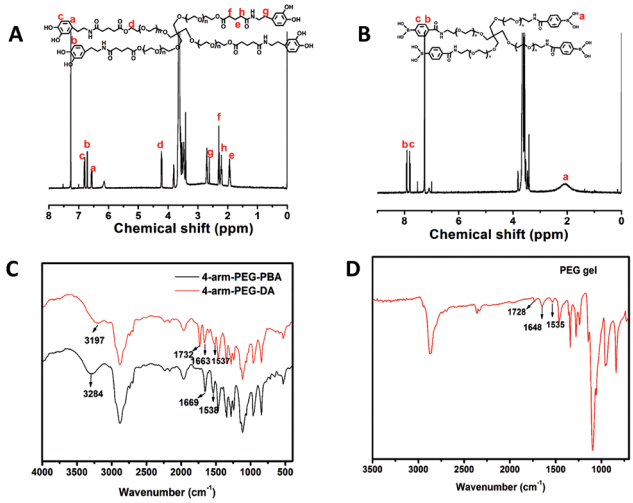

Fig. 2 Characterization of polymers: (1) ^{1}H-NMR spectra of 4-arm-PEG-DA (A) and 4-arm-PEG-PBA (B) in $CDCl_3$; (2) FT-IR spectra of 4-arm-PEG-DA and 4-arm-PEG-PBA (C); (3) ATR-FTIR spectra of PEG hydrogels after lyophilization (D).

ful synthesis of 4-arm-PEG-DA. The proportion of the integral areas of peaks at 6.5 (a) and 4.25 (d) ppm was calculated to be approximately 1 : 1, which demonstrates that almost all ends of 4-arm-PEG were modified with dopamine. In the ^{1}H-NMR spectrum of 4-arm-PEG-PBA (Fig. 2B), the appearance of peaks at 2.1 (a), 7.9 (b) and 7.8 (c) ppm suggests that the 4-arm-PEG-PBA was successfully prepared. The disappearance of the peak at 2.9 ppm, which was the chemical shift of the methylene group near the end of 4-arm-PEG-NH_2 (Fig. S1†), demonstrates the complete conversion from 4-arm-PEG-NH_2 to 4-arm-PEG-PBA. Fig. 2C shows the FT-IR spectra of 4-arm-PEG-DA and 4-arm-PEG-PBA. The typical amide I and II bands at 1663 cm^{-1} ($\nu_{C=O}$) and 1537 cm^{-1} ($\nu_{C(O)-NH}$) observed in Fig. 2C also confirmed the successful synthesis of 4-arm-PEG-DA. The band at 1732 cm^{-1} is ascribed to the vibration absorption of the carboxyl groups of the ester bonds in 4-arm-PEG-DA. The bands at 3197 cm^{-1} and 3284 cm^{-1} are the vibration absorptions of their hydroxyl groups, respectively. Fig. 2D shows the spectrum of the PEG hydrogel after lyophilization. The disappearance of the vibration absorptions of hydroxyl groups indicates the successful formation of the phenylborate ester.

3.2. pH responsive degradation of hydrogels

Phenylborate ester bonds are formed under alkaline conditions and broken at low pH values. Fig. 3A shows the degradation behaviors of hydrogels at different pH values. In particular, the hydrogels were completely degraded within 30 min at pH 3.0. As shown in Fig. 3A, the hydrogels degraded more slowly at pH 9.0 compared to pH 5.0. The degradation time at pH 9.0 and pH 5.0 was 4 h and 2.5 h, respectively. However, at pH 7.4, the hydrogels firstly swelled and then began to degrade after three hours. This was due to the fact that the swelling rate was greater than the degradation rate for initial several hours; however, the swelling rate became smaller than the degradation rate as the time progressed. There was no swelling observed at pH 5.0 and pH 9.0 due to a greater degradation rate than the swelling rate throughout the degradation process. Additionally, as investigated by FT-IR spectra (Fig. 3B), the degradation mechanism of hydrogels in alkaline buffer was different from that in acidic buffer. As shown in Fig. 3B, three bands in the spectrum of degradation products at pH 5.0 including the typical amide vibration absorptions (1659 cm^{-1} and 1539 cm^{-1}) and the vibration absorption of carboxyl groups in ester bonds (1732 cm^{-1}) still existed, suggesting that no other bonds were broken. Although the same three bands also existed in the spectrum of degradation products at pH 9.0, the intensity of the vibration absorption of carboxyl groups in ester bonds (1732 cm^{-1}) was weakened compared to that of carboxyl groups in amide bonds (1659 cm^{-1}) indicating that part of ester bonds were broken under alkaline conditions. However, the intensity of the band at 1732 cm^{-1} was stronger than that at 1659 cm^{-1} in the FT-IR spectra of both 4-arm-PEG-DA and degradation products at pH 5.0. Therefore, the hydrogel could degrade at lower pH or higher pH conditions due to the disruption of phenylborate ester bonds or ester bonds, respectively. At pH 7.4, both phenylborate ester bonds and ester bonds are broken slowly and the hydrogel is relatively stable.

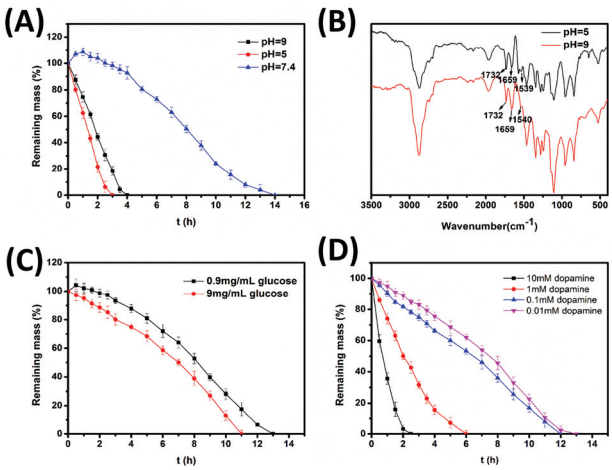

Fig. 3 The degradation behavior of hydrogels at 37 °C: (A) pH responsive degradation of hydrogels; (B) mechanisms of degradation at different pH values; (C) glucose responsive degradation of hydrogels; (D) dopamine responsive degradation of hydrogels.

Published on 13 April 2017. Downloaded on 10/1/2025 12:23:07 AM.

3.3. Glucose responsive degradation of hydrogels

The glucose level in normal human body is 0.7–1.4 mg mL^{-1}.[48] Therefore, the glucose solutions at concentrations of 0.9 mg mL^{-1} and 9 mg mL^{-1} were chosen to mimic normal body and hyperglycemia of diabetes patients, respectively. The glucose has a molecular structure of vicinal diol and can theoretically react with 4-arm-PEG-PBA to form phenylborate ester. In fact, the pK_a of glucose is greater than catechol, implying that it is more difficult to be ionized than catechol.[1,14] Hence, as Fig. 3C shows, there is no significant difference between the degradation behavior of hydrogels in glucose solutions of 0.9 mg mL^{-1} and that at pH 7.4. The hydrogels in more concentrated glucose solutions degraded slightly faster due to the breakage of dynamic phenylborate ester bonds.

3.4. Dopamine responsive degradation of hydrogels

Some mental diseases have a close relationship with the abnormal dopamine level, thus the dopamine-responsive materials provide a potential therapy for these diseases. The dopamine level in the human body does not have a precise value. However, a few researchers have reported that the content of dopamine in the orbitofrontal cortex of rats is 7000 ng g^{-1}.[49] Fig. 3D shows the degradation behaviors of hydrogels in dopamine solutions at different concentrations. The degradation of the hydrogels accelerated with an increasing concentration of dopamine. The degradation time was 2.5 h when the hydrogels were immersed in 10 mM dopamine.

3.5. Rheological studies

Rheology is commonly used to investigate the viscoelastic properties of materials. Fig. 4 shows the rheological behavior of the PEG hydrogel. At high frequency, G' is significantly higher than the G'' value and the hydrogel behaves increasingly elastically as the frequency increases, indicating the formation of covalently cross-linked networks.[50] The long polymer chains between cross-links probably do not get the opportunity to rearrange themselves within the short time scale of the imposed deformation and hence, these networks stiffened and exhibited elevated G' values. The increased G'' at low frequency demonstrates the elevated viscous dissipation due to the presence of reversible bonds in the hydrogel network,[43,51–53] suggesting a good adhesive property of hydrogels. The resulting values of G' and G'' in experiments were much higher (>10-fold) than those of the hydrogels formed by catechol-Fe^{3+} interactions.[5,12]

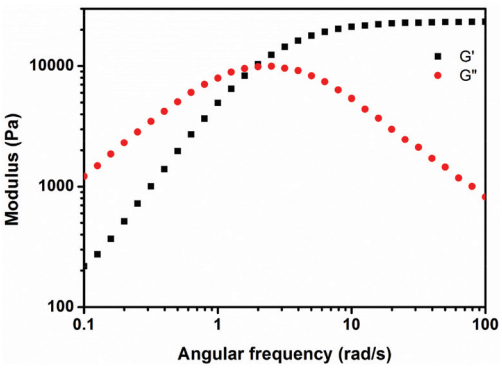

Fig. 4 Rheological behavior of PEG hydrogels.

3.6. Cross-sectional morphology of hydrogels

Fig. 5 shows the cross-sectional morphology of hydrogels. The porous structures with a pore size of dozens of micrometers were observed in the lyophilized hydrogel, which was suitable for the entrapment and transportation of drugs and cell growth.

3.7. Self-healing properties of hydrogel

As shown in Fig. 6, the two pieces of fractured hydrogels were brought into contact with each other and they self-healed to form a single complete piece of hydrogel within 30 s. As shown in the fourth photograph, the joint was strong enough to be stretched.

3.8. *In vitro* triple responsive rhodamine B release behavior from hydrogels

Rhodamine B is widely used as a dye in industries and laboratories. However, due to its carcinogenic activity,[54,55] rhodamine B has not been used as a food color for several years. In the current work, rhodamine B was selected as a model drug because of its good water solubility, convenient detection, and negligible influence on the hydrogel formulation. Fig. 7A shows the cumulative drug release from the hydrogels at different pH values. The results showed that rhodamine B released at the fastest rate at pH 5.0 and at the slowest rate at pH 7.4, which was due to the breakage of phenylborate ester bonds under acidic conditions. The hydrogels took approximately 5 hours at pH 5.0 to degrade completely while the

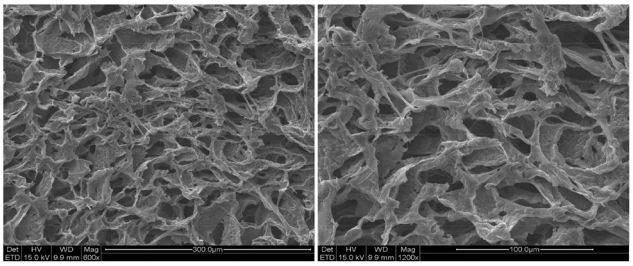

Fig. 5 The SEM images of the cross-section of lyophilized hydrogels.

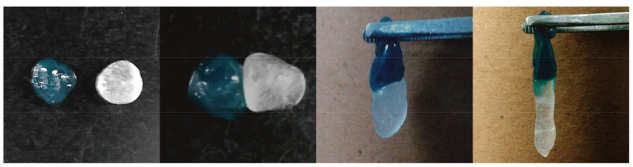

Fig. 6 The photographs of self-healing properties of hydrogels. One piece of hydrogel was dyed with methylene blue.

 This journal is © The Royal Society of Chemistry 2017

Published on 13 April 2017. Downloaded on 10/1/2025 12:23:07 AM.

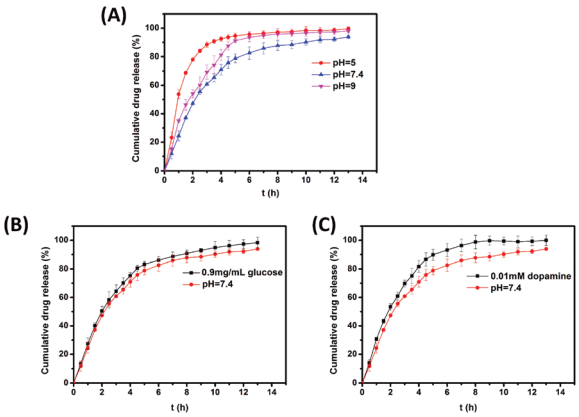

Fig. 7 The release profiles of rhodamine B from hydrogels under different conditions.

degradation time at pH 7.4 was much longer. Fig. 7B shows the cumulative drug release from hydrogels in glucose solutions. A high concentration of glucose can accelerate the release of rhodamine B. Fig. 7C indicates that small dopamine molecules in solution can accelerate the drug release.

3.9. Lap shear strength tests

Lap shear strength experiments were performed to determine the adhesive properties of hydrogels. The hydrogels were applied to porcine dermal tissue substrates attached to glass slides. As is shown in Fig. 8, the mean shear strength of the adhesive hydrogel on porcine dermal tissue substrates was 5.2 ± 0.28 kPa. The measured value was higher than the previously reported values for the hydrogels formed by the oxidation of catechol (1.01 ± 0.09 kPa).[56] The hydrogels were also tested after self-healing and the results are exhibited in Fig. 8b. The lap shear strength of hydrogels after self-healing did not decrease by a large amount (5.07 ± 0.35 kPa). Moreover, the PEG hydrogels also had a good adhesion to glass slides. The mean shear strength of hydrogels on glass slides before and after self-healing was 4.09 ± 0.34 kPa and 3.97 ± 0.24 kPa, respectively. Hence, it could be concluded that the PEG hydrogel has a better adhesion to bio-tissues and can be potentially used as an adhesive. Fig. 8c provides another proof of adhesion of hydrogels on glass slides. A weight of 200 g can be firmly adhered to the glass slides by the PEG hydrogel both before and after self-healing. In this system, the good adhesion of hydrogels to glass slides was due to the hydrogen bonding between the hydroxyl groups in hydrogels (catechol, phenylboronic acid and phenylborate esters) and Si-OH. The excellent adhesion to porcine skin resulted from the hydrogen bonding between the hydrogel and the hydroxyl, amino and carboxyl groups on the porcine skin. In addition, π–π stacking may also play a certain role in the adhesion to porcine skin since the aromatic rings existed in the hydrogel and porcine skin.

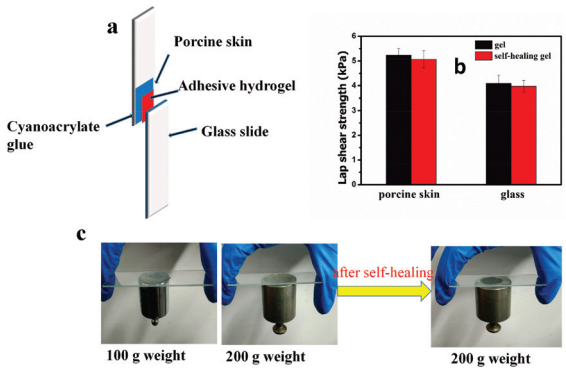

Fig. 8 (a) Schematic illustration of lap shear strength tests; (b) lap shear strength results of hydrogels before and after self-healing; (c) photos of the adhesion properties of hydrogels on glass slides.

3.10. *In vitro* cytotoxicity tests

The cytotoxicity of PEG hydrogels to L929 cells was assessed by the MTT assay and the results are shown in Fig. 9. The results showed that hydrogel extracts were noncytotoxic, with a relative cell viability of more than 70%. Fig. 9 shows that even the non-diluted extracts after incubation for 24 h were nontoxic. The 15 wt% 4-arm-PEG-DA and 15 wt% 4-arm-PEG-PBA solutions were also found to be noncytotoxic. The results indicate that the hydrogels had an excellent cytocompatibility and could be potentially utilized as a biomedical material.

3.11. Cell growth on the surface of hydrogels

AO can pass through the unbroken membrane of cells to combine with DNA of the nucleus to generate green fluorescence. But EB can only enter cells with damaged cell membranes to emit stronger orange fluorescence. The combination of AO and EB can be utilized to distinguish between the live cells and the dead cells roughly.

Fig. 10 shows the results of these experiments. Exclusively, green fluorescence was observed in all images, suggesting that the cells grew well on the surface of hydrogels. Additionally,

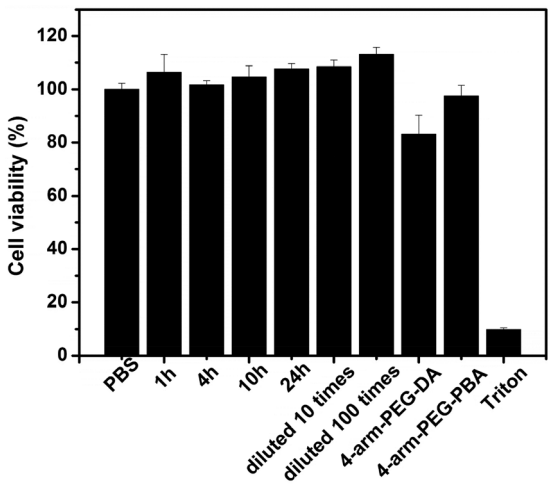

Fig. 9 *In vitro* cytotoxicity of hydrogel extracts and precursor polymer solutions to L929 cells. The cells were incubated at 37 °C for 48 h.

Published on 13 April 2017. Downloaded on 10/1/2025 12:23:07 AM.

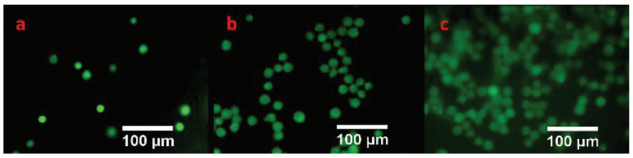

Fig. 10 Fluorescence images of L929 cells cultured on the surface of hydrogels for 0 (a), 1 (b), and 2 (c) days.

the number of cells increased over time, revealing that the hydrogel was conductive to cell growth and reproduction.

4. Conclusions

In the current work, a pH, glucose, and dopamine triple responsive PEG hydrogel was successfully developed by the formation of phenylborate–catechol complexation. It should be noted that this is the first reported work of dopamine-responsiveness. The dynamic covalent bond bestowed self-healing properties to the hydrogel, and in the process improved its working life. The values of G' and G'' of the hydrogel were higher than that of other reported polymeric hydrogels. The measurements of lap shear strength indicate that the hydrogel had a strong adhesion to bio-tissues and *in vitro* cytotoxicity tests demonstrate the excellent cytocompatibility of hydrogels. In conclusion, the formulated hydrogel has potential applications in biomedical fields as a multi-responsive drug delivery system and a self-healable bio-adhesive.

Acknowledgements

This work was funded by the Natural Science Foundation of Tianjin (14JCYBJC18100), the NSFC (51203079), and the PCSIRT (IRT1257).

Notes and references

1 L. He, D. E. Fullenkamp, J. G. Rivera and P. B. Messersmith, *Chem. Commun.*, 2011, **47**, 7497–7499.
2 I. Strehin, Z. Nahas, K. Arora, T. Nguyen and J. Elisseeff, *Biomaterials*, 2010, **31**, 2788–2797.
3 T. Sakai, T. Matsunaga, Y. Yamamoto, C. Ito, R. Yoshida, S. Suzuki, N. Sasaki, M. Shibayama and U. Chung, *Macromolecules*, 2008, **41**, 5379–5384.
4 J. D. Ehrick, M. R. Luckett, S. Khatwani, Y. Wei, S. K. Deo, L. G. Bachas and S. Daunert, *Macromol. Biosci.*, 2009, **9**, 864–868.
5 N. Holten-Andersen, M. J. Harrington, H. Birkedal, B. P. Lee, P. B. Messersmith, K. Y. C. Lee and J. H. Waite, *Proc. Natl. Acad. Sci. U. S. A.*, 2011, **108**, 2651–2655.
6 J. H. Ryu, Y. Lee, W. H. Kong, T. G. Kim, T. G. Park and H. Lee, *Biomacromolecules*, 2011, **12**, 2653–2659.
7 I. Tomatsu, K. Peng and A. Kros, *Adv. Drug Delivery Rev.*, 2011, **63**, 1257–1266.
8 Y. Zhou, J. Zhao, X. Sun, S. Li, X. Hou, X. Yuan and X. Yuan, *Biomacromolecules*, 2016, **17**, 622–630.
9 S. Lee, Y. H. Park and C. S. Ki, *Int. J. Biol. Macromol.*, 2016, **83**, 1–8.
10 C. Cha, E. Antoniadou, M. Lee, J. H. Jeong, W. W. Ahmed, T. A. Saif, S. A. Boppart and H. Kong, *Angew. Chem., Int. Ed.*, 2013, **125**, 7087–7090.
11 C. T. Huynh, M. K. Nguyen, D. P. Huynh, S. W. Kim and D. S. Lee, *Polymer*, 2010, **51**, 3843–3850.
12 M. Cencer, M. Murley, Y. Liu and B. P. Lee, *Biomacromolecules*, 2015, **16**, 404–410.
13 M. Cencer, Y. Liu, A. Winter, M. Murley, H. Meng and B. P. Lee, *Biomacromolecules*, 2014, **15**, 2861–2869.
14 V. Yesilyurt, M. J. Webber, E. A. Appel, C. Godwin, R. Langer and D. G. Anderson, *Adv. Mater.*, 2016, **28**, 86–91.
15 B. V. Farahani, H. Ghasemzadeh and S. J. Afraz, *J. Chin. Chem. Soc.*, 2016, **63**, 438–444.
16 M. Nakahata, S. Mori, Y. Takashima, H. Yamaguchi and A. Harada, *Chem.*, 2016, **1**, 766–775.
17 L. Si, X. Zheng, J. Nie, R. Yin, Y. Hua and X. Zhu, *Chem. Commun.*, 2016, **52**, 8365–8368.
18 T. Ichi, J. Watanabe, T. Ooya and N. Yui, *Biomacromolecules*, 2001, **2**, 204–210.
19 Y. Okumura and K. Ito, *Adv. Mater.*, 2001, **13**, 485–487.
20 T. Karino, Y. Okumura, C. Zhao, T. Kataok, K. Ito and M. Shibayama, *Macromolecules*, 2005, **38**, 6161–6167.
21 Q. Li, D. G. Barrett, P. B. Messersmith and N. Holten-Andersen, *ACS Nano*, 2016, **10**, 1317–1324.
22 B. P. Lee and S. Konst, *Adv. Mater.*, 2014, **26**, 3415–3419.
23 K. Kataoka, H. Miyazaki, M. Bunya, T. Okano and Y. Sakurai, *J. Am. Chem. Soc.*, 1998, **120**, 12694–12695.
24 Y. Guan and Y. Zhang, *Chem. Soc. Rev.*, 2013, **42**, 8106–8121.
25 G. Deng, C. Tang, F. Li, H. Jiang and Y. Chen, *Macromolecules*, 2010, **43**, 1191–1194.
26 T. L. Nguyen, T. H. Nguyen, C. K. Nguyen and D. H. Nguyen, *Biomed. Res. Int.*, 2017, 8589212.
27 W. Zhang, J. Duchet and J. F. Gérard, *RSC Adv.*, 2016, **6**, 114235–114243.
28 P. Sun, J. Wang, X. Yao, Y. Peng, X. Tu, P. Du, Z. Zheng and X. Wang, *ACS Appl. Mater. Interfaces*, 2014, **6**, 12495–12504.
29 C. E. Brubaker, H. Kissler, L. J. Wang, D. B. Kaufman and P. B. Messersmith, *Biomaterials*, 2010, **31**, 420–427.
30 S. Moulay, *Polym. Rev.*, 2014, **54**, 436–513.
31 Y. Liu, K. Ai and L. Lu, *Chem. Rev.*, 2014, **114**, 5057–5115.
32 Y. Lee, H. J. Chung, S. Yeo, C.-H. Ahn, H. Lee, P. B. Messersmith and T. G. Park, *Soft Matter*, 2010, **6**, 977–983.
33 Q. Zhao, D. W. Lee, B. K. Ahn, S. Seo, Y. Kaufman, J. N. Israelachvili and J. H. Waite, *Nat. Mater.*, 2016, **15**, 407–412.
34 L. A. Burzio, *Biochemistry*, 2000, **39**, 11147–11153.
35 Y. Ai, Y. Wei, J. Nie and D. J. Yang, *J. Photochem. Photobiol., B*, 2013, **120**, 183–190.

 This journal is © The Royal Society of Chemistry 2017

Published on 13 April 2017. Downloaded on 10/1/2025 12:23:07 AM.

36 L. Q. Xu, W. J. Yang, K.-G. Neoh, E.-T. Kang and G. D. Fu, *Macromolecules*, 2010, **43**, 8336–8339.
37 G. Barany, N. Kneib-cordonier and D. G. Mullen, *Int. J. Pept. Protein Res.*, 1987, **30**, 705–739.
38 B. P. Lee, J. L. Dalsin and P. B. Messersmith, *Biomacromolecules*, 2002, **3**, 1038–1047.
39 C. Nam, T. J. Zimudzi, G. M. Geise and M. A. Hickner, *ACS Appl. Mater. Interfaces*, 2016, **8**, 14263–14270.
40 Y. Arai and D. L. J. Sparks, *J. Colloid Interface Sci.*, 2001, **241**, 317–326.
41 K. J. Howe, K. P. Ishida and M. M. Clark, *Desalination*, 2002, **147**, 251–255.
42 C. E. Brubaker and P. B. Messersmith, *Biomacromolecules*, 2011, **12**, 4326–4334.
43 Y. Liu, H. Meng, S. Konst, R. Sarmiento, R. Rajachar and B. P. Lee, *ACS Appl. Mater. Interfaces*, 2014, **6**, 16982–16992.
44 B. J. Kim, D. X. Oh, S. Kim, J. H. Seo, D. S. Hwang, A. Masic, D. K. Han and H. J. Cha, *Biomacromolecules*, 2014, **15**, 1579–1585.
45 ISO 10993–5: Biological evaluation of medical devices. In part 5: Tests for cytotoxicity: in vitro methods; International organization for standardization: 2012.
46 M. Mehdizadeh, H. Weng, D. Gyawali, L. Tang and J. Yang, *Biomaterials*, 2012, **33**, 7972–7983.
47 R. E. Kerby, A. Tiba, B. M. Culbertson, S. Schricker and L. J. Knobloch, *Macromol. Sci. A*, 1999, **36**, 1227–1239.
48 M. J. Lanspa, E. Hirshberg, A. M. Hersh, J. Holmen, J. Orme, A. Morris and J. S. Krinsley, *Am. J. Respir. Crit. Care Med.*, 2016, **193**, A3652.
49 S. Wu, S. An, H. Chen and F. Li, *Acta Psychol. Sin.*, 2014, **46**, 69–78.
50 S. Skelton, M. Bostwick, K. O'Connor, S. Konst, S. Casey and B. P. Lee, *Soft Matter*, 2013, **9**, 3825–3833.
51 J. Yang, C.-R. Han, X.-M. Zhang, F. Xu and R.-C. Sun, *Macromolecules*, 2014, **47**, 4077–4086.
52 T. Narita, K. Mayumi, G. Ducouret and P. Hébraud, *Macromolecules*, 2013, **46**, 4174–4183.
53 S. Rose, A. Marcellan, D. Hourdet, C. Creton and T. Narita, *Macromolecules*, 2013, **46**, 4567–4574.
54 J. Anandkumar and B. J. Mandal, *Hazard. Mater.*, 2011, **186**, 1088–1096.
55 M. Sivakumar and A. B. Pandit, *Ultrason. Sonochem.*, 2001, **8**, 233–240.
56 J. Xu, G. M. Soliman, J. Barralet and M. Cerruti, *Langmuir*, 2012, **28**, 14010–14017.